to test whether the fluorination reaction was reversible, sample 2 was reannealed under O_2 at 900 °C followed by slow cooling to give sample 3. Sample 3 was analyzed for fluorine. Calcd for $YBa_2Cu_3F_{1.4}O_{6.5}$ (found): F, 3.88 (F, 3.23, 4.22). Superconductivity was again observed in sample 3 with a sharp onset at 93 K, followed by a long tail that did not vanish until 65 K. Powder X-ray data revealed that a significant amount of F has been converted to BaF_2 at this stage, and sample 3 appears to be a mixture of 1:2:3 perovskite and BaF_2.

Since molecular fluorine reacted readily with the tetragonal 1:2:3 perovskite, we also carried out fluorination of the orthorhombic $YBa_2Cu_3O_{6.8}$ sample. The material was exposed to 1 atm of a 20% v/v mixture of F_2 in O_2. Reaction for 2 h at 280 °C led to the introduction of 1 equiv of fluorine atoms/mol and evolution of about 0.5 equiv of O/mol as O_2 (sample 4). This sample was analyzed for fluorine. Calcd for $YBa_2Cu_3F_{0.8}O_{6.5}$ (found): F, 2.26 (F, 2.24, 2.05). The powder pattern of sample 4 appeared to be orthorhombic and gave no evidence for the presence of BaF_2. Interestingly, all the (001) peaks were much stronger than those of the typical orthorhombic phase, which was indicative of preferred orientation. However, sample 4 is semiconductive throughout the temperature range we measured (300–15 K). Recently, a T_c of 148.5 K was reported from "low dosage" fluorine ions implantation (no composition given) of $YBa_2Cu_3O_x$.[21] We, therefore, prepared a specimen of low fluorine content, sample 5, by treating the orthorhombic form of $YBa_2Cu_3O_{6.8}$ at 300 °C with a small amount of F_2 in 1 atm of O_2. Sample 5 was analyzed for fluorine. Calcd for $YBa_2Cu_3F_{0.15}O_{6.5}$ (found): F, 0.43 (F, 0.40, 0.43). The resistivity curve showed a slight increase in resistance with decreasing temperature and a sharp T_c near 92 K. Thus, superconductivity near 90 K was only observed in samples of low fluorine content, which is consistent with our previous results.

Conclusions. We have demonstrated that when barium fluoride is mixed with Y_2O_3, CuO, and $BaCO_3$ in an attempt to introduce fluorine into the 1:2:3 perovskites, 95 ± 5% of the BaF_2 remains unreacted throughout the firing process. Use of copper and yttrium fluorides leads to similar results, since CuF_2 and YF_3 are readily converted to BaF_2 in the presence of $BaCO_3$. The superconductivity observed near 93 K in some samples is likely caused solely by the well-known orthorhombic perovskite, $YBa_2Cu_3O_{6.8}$. In the fluorine gas experiments in which F_2 reacted with either the oxygen-deficient tetragonal phase $YBa_2Cu_3O_x$ ($x \leq 6.5$), or the orthorhombic phase $YBa_2Cu_3O_{6.8}$, the results are consistent with actual fluorine incorporation. Finally, there is no sign of any drop in resistivity between 300 and 93 K for any of our samples, indicating that under the conditions given herein there is *no* superconducting F-containing phase formed with $T_c \simeq 155$ K.

Experimental Section. $YBa_2Cu_3O_{6.8}$ was prepared according to a literature procedure.[4] All chemicals were reagent grade or better. Fluorine analyses were carried out by Midwest Microlab, Indianapolis, IN. The formula, $YBa_2Cu_3F_xO_{6.5}$, was used to calculate the weight percentage of fluorine in all the fluorine gas experiments. Conductivities of sintered pellets were measured by using standard four probe techniques with ac currents and phase-sensitive detection. Currents of ~500 μA at a frequency of ~99 Hz were used.

The ^{19}F NMR spectra were recorded on two different spectrometers to minimize the chance of systematic error. One was a Bruker Instruments Model AM300, operating at a ^{19}F resonance frequency of 282.4 MHz. The other was a Nicolet Magnetics Model NTC-200, operating at a ^{19}F resonance frequency of 188.2 MHz, with an Andrews' design "magic"-angle sample-spinning solids probe. Typical operating parameters were a 90° pulse of 5 μs, a spectral width of ±62 kHz, a pulse recycle time of 500 s, and a total accumulation of 32 transients. Sample spinning speeds varied between 0 and 3 kHz.

Introduction of F_2 was carried out in a metal fluorine-handling vacuum line. The sample was contained in an alumina boat placed in a preconditioned nickel reaction vessel. Reaction was monitored by observing pressure changes with a Monel Bourdon gauge and also with an on-line quadrupole mass spectrometer. Molecular fluorine was always the limiting reagent, and reaction was continued until the F_2 was completely or nearly completely consumed.

Acknowledgment. Work at Argonne National Laboratory is sponsored by the Office of Basic Energy Science, Divisions of Materials and Chemical Sciences, U.S. Department of Energy (DOE), under Contract W-31-109-ENG-38. M.Y.C., J.A.S., B.D.G., S.L.H., and A.M.D. are student research participants sponsored by the Argonne Division of Educational Programs from the University of Illinois (Urbana-Champaign, IL), Valparaiso University (Valparaiso, IN), Northern Illinois University (DeKalb, IL), Wellesley College (Wellesley, MA), and St. Ignatius High School (Chicago, IL), respectively.

Chemistry and Materials Science Divisions
Argonne National Laboratory
Argonne, Illinois 60439

Hau H. Wang*
Aravinda M. Kini
Huey-Chuen I. Kao
Evan H. Appelman
Arthur R. Thompson
Robert E. Botto
K. Douglas Carlson
Jack M. Williams*
Marilyn Y. Chen
John A. Schlueter
Bradley D. Gates
Susan L. Hallenbeck
Andrea M. Despotes

Received October 2, 1987

(21) Meng, X.-R.; Ren, Y.-R.; Lin, M.-Z.; Tu, Q.-Y.; Lin, Z.-J.; Sang, L.-H.; Ding, W.-Q.; Fu, M.-H.; Meng, Q.-Y.; Li, C.-J.; Li, X.-H.; Qiu, G.-L.; Chen, M. Y. *Solid State Commun.* **1987**, *64*, 325.

Chemical Vapor Deposition of $FeCo_x$ and $FeCo_xO_y$ Thin Films from Fe–Co Carbonyl Clusters

Sir:

Chemical vapor deposition (CVD) is a process widely used to prepare thin films finding diverse technical applications.[1] This chemical process involves the reaction of vapor-phase constituents near or on a heated substrate to produce a solid film and gaseous product species. Classical CVD is limited by the relatively high temperatures typically required and the inability to prepare many desired phases. The use of organometallic compounds as vapor-phase reagents can circumvent the high-temperature limitations, but relatively few organometallic compounds have been studied, and the extent of applicability of these compounds is not known.[2] Particularly difficult to prepare by any CVD technique are mixed-metal alloy and oxide thin films, of which the latter are particularly interesting because of their magnetic properties.[3] One potential route to such films is to vapor-deposit preformed mixed-metal organometallic clusters, a method that should yield homogeneous deposits. Herein, we describe the use of the heteronuclear carbonyl clusters $HFeCo_3(CO)_{12}$[4] and $CpFeCo(CO)_6$[5] to form mixed-metal Fe/Co alloy and oxide thin films using the CVD reactor shown in Figure A of the supplementary material.[6,7]

(1) Powell, C. F.; Oxley, J. H.; Blocher, J. M. *Vapor Deposition*; Wiley: New York: 1966.
(2) (a) Bryant, W. A. *J. Mater. Sci.* **1975**, *11*, 48. (b) For a recent excellent example of an organometallic CVD route to TiC films, see: Girolami, G. S.; Jensen, J. A.; Pollina, D. M.; Williams, W. S.; Kaloyeros, A. E.; Allocca, C. M. *J. Am. Chem. Soc.* **1987**, *109*, 1579.
(3) Thompson, J. E. *The Magnetic Properties of Materials*; CRC: London, 1968.
(4) Chini, P.; Colli, L.; Peraldo, M. *Gazz. Chim. Ital.* **1960**, *90*, 1005.
(5) Madach, T.; Vahrenkamp, H. *Chem. Ber.* **1980**, *113*, 2675.

0020-1669/88/1327-0008$01.50/0

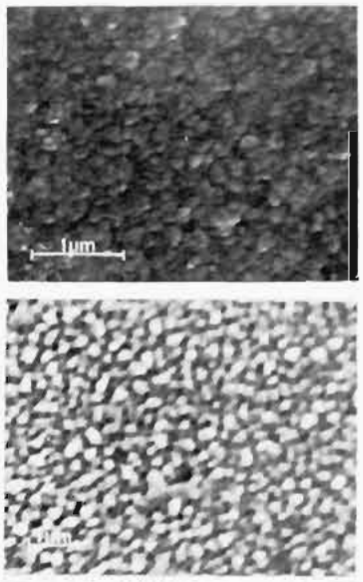

Figure 1. SEM of (top) $HFeCo_3(CO)_{12}$-derived Fe/Co thin film (57 800×) and (bottom) $CpFeCo(CO)_6$-derived Fe/Co thin film (19 500×).

The above Fe/Co clusters consistently gave thin metallic films on glass substrates when vaporization temperatures 5–10 °C below the melting points of the organometallics $HFeCo_3(CO)_{12}$, 85 °C; $CpFeCo(CO)_6$, 52 °C), deposition temperatures in the 300–350 °C range, and CO as carrier gas with a 30–50 cm^3/min flow rate were used. These conditions typically gave films with thicknesses of 0.8–1.5 μm and deposition rates in the range of 0.1–0.15 μm/h. The temperature in the deposition zone is critical in this process. At temperatures below 300 °C, the deposition rate was too slow to be practical, whereas deposition at temperatures in excess of 350 °C resulted in nucleation in the gas phase above the glass slide and formation of a poorly adhering sootlike coating. Vaporization temperatures higher than those used gave extensive decomposition in the vaporization flask, but this was minimized by using CO as a carrier gas and the specified temperatures. N_2, H_2, and He carrier gases gave inferior results. Flow rates higher than those used gave deposition only on the edges of the substrate.

Mixed-metal oxide films were prepared in a similar way either by introduction of oxygen into the flow system downstream of the vaporization vessel during the deposition process or by posttreatment of heated (300–350 °C) mixed-metal films with oxygen gas. In either case, rust-colored films were produced with film thicknesses in the same range as the metallic films. These films were metallic in appearance, uniform, adhering, and nonconducting.

Representative SEM micrographs of the metal films are shown in Figure 1. These show the formation of uniform films with a granular surface composed of particles 700–1000 μm in size in the $HFeCo_3(CO)_{12}$-derived films and 3000–5000 μm in size in the $CpFeCo(CO)_6$-derived films. The absence of observable lines in the X-ray powder diffraction spectra suggests that the films are amorphous. EDAX analysis showed that both Fe and Co were present in the films, and metal mapping indicated an even dispersion of these elements throughout the films. Although metallic in appearance, the films were only slightly conducting. Scratch and Scotch tape testing of the surface of the films showed them to be coherent and adherent. X-ray powder diffraction of the oxide films showed them to be amorphous, and EDAX analysis showed the homogeneous distribution of both Fe and Co.

Table I. Representative Elemental Ratios of Iron and Cobalt

precursor	theor Fe/Co ratio	exptl Fe/Co ratio[a]
	Metal Films	
$HFeCo_3(CO)_{12}$	0.33	0.50
$CpFeCo(CO)_6$	1.00	1.20
	Oxide Films	
$HFeCo_3(CO)_{12}$	0.33	0.40
$CpFeCo(CO)_6$	1.00	1.19

[a] By atomic absorption analysis;[8] average of three runs.

The ratios of metals present in the films as determined by atomic absorption analysis are summarized in Table I.[8] Both the $CpFeCo(CO)_6$- and $HFeCo_3(CO)_{12}$-derived films are iron-rich, by approximately 20% and 50%, respectively. These percentages reflect the tendency of the starting materials to thermally decompose in the vaporization flask to yield volatile organoiron complexes and less volatile Co species.[9] The observed ratios do qualitatively reflect the stoichiometry in the starting compounds, and these ratios would presumably approach the theoretical values if lower vaporization temperatures were used. The latter would necessitate longer deposition times, but that could be offset by running the depositions at reduced pressures. Elemental analyses did not detect any carbon in a $HFeCo_3(CO)_{12}$-derived film, and only 0.05% was detected in films prepared from $CpCoFe(CO)_6$.[9] Electron microprobe analysis of the metallic films showed that no detectable oxide phases were present, in contrast to the case for films exposed to oxygen, for which the presence of both Fe^{3+} and Co^{2+} oxides was indicated.[10]

Preliminary investigations into the saturation magnetization of the $HFeCo_3(CO)_{12}$-derived alloy films indicate that they are ferromagnetic, with a saturation magnetization, σ_{sat}, of 102 emu/g.[12] This value translates into a saturation moment, μ_{sat}, of 4.26, significantly greater than the value of 2.0 predicted by the Slater–Pauling curves.[13] Further study of this phenomenon is now being carried out.

(6) Kaplan, Y.; Belysheva, G. V.; Zhipsov, S. F.; Domrachev, G. A.; Chernyshava, L. S. *Zh. Obshch. Khim.* **1980**, *50*, 118.

(7) For each experimental run, a glass microscope slide was positioned in a resistively heated deposition zone in a glass chamber so as to be in line with the inlet tube. The system was evacuated to 10^{-3} mmHg while the deposition chamber and inlet line were heated to their respective temperatures. The carrier gas was then introduced into the system at the chosen flow rate. After temperature stabilization, the metal cluster (50–100 mg) was introduced into a vaporization flask through which the carrier gas flows. After brief evacuation, the carrier gas was metered into the system, and the vaporization flask was heated to the vaporization temperature. Each run lasted between 6 and 12 h. Additional reactant or diluent gases were introduced into the deposition chamber only after consistent flow rate and temperatures were maintained. Posttreatment of the films with O_2 was carried out in the same apparatus.

(8) Standard solutions were prepared by dissolving $Co_2(CO)_8$, $[CpFe(CO)_2]_2$, and iron and cobalt powders in a mixture of 5 mL of concentrated HCl and 10 mL of HNO_3 and then diluting to 1000 mL. The deposited films were dissolved from the glass slides by using the same solution of acid.

(9) A study of the thermal decomposition behavior of $HFeCo_3(CO)_{12}$ and $CpFeCo(CO)_6$ at their melting points under a CO atmosphere indicates that the following reactions occur:

$$4HFeCo_3(CO)_{12} + 8CO \rightarrow 4Fe(CO)_5 + 3Co_4(CO)_{12} + H_2 \quad (1)$$

$$2CpFeCo(CO)_6 + xCO \rightarrow [CpFe(CO)_2]_2 + Co_y(CO)_z \quad (2)$$

The cobalt product in eq 2 is likely a decomposition product of $Co_2(CO)_8$.

(10) Elemental analyses for carbon were conducted by Schwartzkopf Microanalytical Laboratories, Woodside, NY.

(11) Oxygen analyses were carried out on an electron microprobe instrument, using a reference library of known oxide phases.

(12) Magnetic measurements were carried out by using a vibrating-sample magnetometer (VSM). Samples were approximately 0.003-g films deposited on preweighed glass slides. Measurements were made at room temperature and a field strength of 8 kOe.

(13) Morrish, A. H. *Physical Principles of Magnetism*; Wiley: New York, 1965.

(14) (a) A recent patent[11b] has claimed the formation of Fe/Co films by CVD using $[Co((CH_3)_2CO)_6][FeCo_3(CO)_{12}]_2$. Only oxide and carbide phases were formed when they were deposited with CO as a carrier gas and there was a perfect agreement between the determined Fe/Co ratio and that expected on the basis of the composition of the organometallic compound. (b) Cornils, B.; Tihanyi, B.; Weber, J.; DeWin, W.; Erbin, E.; Muhlratzer, A. (Ruhrchemie Aktiengesellshaft; Maschinenefabrik Augsburg-Nurnberg) U.S. Patent 4 510 182, April 9, 1985.

This work has demonstrated that homogeneous mixed-metal alloy and oxide films can be prepared by the chemical vapor deposition of Fe/Co heteronuclear organometallic clusters. This technique should in principle be extendable to clusters of various metal compositions so as to give a wide range of metal and oxide phases.[11]

Acknowledgment. We thank Dr. K. Spear and Dr. R. Messier of the Materials Research Laboratory for invaluable discussions on CVD, apparatus design, and film characterization and D. Strickler, L. Eminhizer, and N. Suhr for assistance in SEM, electron microprobe, and atomic absorption analyses, respectively. We also thank Dr. L. N. Mulay for his assistance in making and interpreting the magnetic measurements.

Supplementary Material Available: A drawing of the experimental CVD apparatus (Figure A) (1 page). Ordering information is given on any current masthead page.

Department of Chemistry
The Pennsylvania State University
University Park, Pennsylvania 16802

Corinna L. Czekaj*
Gregory L. Geoffroy*

Received October 7, 1987

Articles

Contribution from the Department of Chemistry, Université du Québec à Montréal, C.P. 8888, succ. A, Montréal, Canada H3C 3P8

Crystal Structure of a Hydroxo-Bridged Platinum(II) Tetramer, *cyclo*-Tetrakis(μ-hydroxo)tetrakis((ethylenediamine)platinum(II)) Tetranitrate

F. D. Rochon,* A. Morneau, and R. Melanson

Received March 19, 1987

The crystal structure of *cyclo*-tetrakis(μ-hydroxo)tetrakis((ethylenediamine)platinum(II)) tetranitrate has been determined by X-ray diffraction. The monoclinic crystal, space group $P2_1/c$, has cell dimensions $a = 9.544$ (4) Å, $b = 17.683$ (14) Å, $c = 16.725$ (18) Å, and $\beta = 92.91$ (6)° with four tetramers in the unit cell. The structure was refined to $R = 0.057$ and $R_w = 0.048$. The cation consists of an eight-membered ring with approximate symmetry S_4. Each platinum in the hydroxo-bridged tetramer has square-planar coordination. The four Pt atoms in the ring are planar with two cross-ring O atoms on one side of the plane and the other two O atoms on the other side. The cross-ring oxygen–oxygen interactions of 2.68 (3) and 2.74 (2) Å seem to indicate intramolecular hydrogen bonding. The crystal is stabilized by an extensive hydrogen-bonding system. All the amine groups are hydrogen-bonded to the nitrate ions.

Introduction

The anticancer drug cisplatin, *cis*-$[Pt(NH_3)_2Cl_2]$, has been shown to bind predominantly to d(GpG) sequences in cellular DNA.[1] The neutrality requirement of the drug is important for its passage through the cell membranes. Inside the cells, where the chloride ion concentration is much lower than in the blood plasma, the complex is hydrolyzed. At physiological pH, the predominant hydrolyzed species is *cis*-$[Pt(NH_3)_2(H_2O)(OH)]^+$, which has been shown to oligomerize quite rapidly.[2] The hydrolyzed products of cisplatin were found by ^{195}Pt NMR studies to contain monomers and hydroxo-bridged dimers and trimers. These oligomeric species are toxic[2] and might be partly responsible for the toxicity of cisplatin.

The crystal structures of the NO_3^- and CO_3^{2-} salts of the planar bis(hydroxo)-bridged dimers have been reported several years ago.[3-5] The crystal structure of the SO_4^{2-} and NO_3^- salts of a trimeric cation were also investigated.[6,7]

Chelates in which the NH_3 ligands have been replaced by 1,2-diaminocyclohexane (dach) seem to show higher antitumor activity than cisplatin with a reduced toxicity. Furthermore, the hydroxo-bridged dimers and trimers of dach–Pt(II) complexes are active anticancer agents and are less toxic than the monomer,[8] in contrast to the case for the NH_3 oligomers. This might partly account for the reduced toxicity of dach complexes. The crystal structure of the SO_4^{2-} salt of a *trans*-dach hydroxo-bridged trimer was recently reported.[9]

The antitumor activity of the chelate complex $[Pt(en)Cl_2]$ (en = ethylenediamine) is well-known. It is also less toxic than cisplatin.[10] The antitumor activity of the hydroxo-bridged dimer of en was determined by Broomhead, Fairlie, and Whitehouse, and the dimer was found to be toxic.[11] The dinuclear platinum(II) complex was prepared by a slight modification of the method used for $[Pt(NH_3)_2OH]_2(NO_3)_2$. The compound was characterized mainly by infrared spectroscopy, which showed the characteristic Pt–O–H bending vibration at 950–1100 cm^{-1}.

We have recently attempted to prepare the hydroxo-bridged dimer of en by a similar method. The elemental analyses and the conductance measurements of the crystallized compound were in agreement with the dimer formulation. We chose one crystal for X-ray diffraction studies. To our surprise, we found that the compound was a hydroxo-bridged cyclic tetramer. Tetramers were suspected to exist in small quantities in solution, but no such compound of platinum(II) has been reported yet. We now report the crystal structure of *cyclo*-tetrakis(μ-hydroxo)tetrakis-((ethylenediamine)platinum(II)) tetranitrate.

Experimental Section

Synthesis. $[Pt(en)Cl_2]$ (1.08 mmol) and $AgNO_3$ (2.14 mmol) were stirred together in 10 mL of water in the dark. After 24 h, the AgCl

(1) Pinto, A. L.; Lippard, S. J. *Biochim. Biophys. Acta* **1985**, *780*, 167–180.
(2) Rosenberg, B. *Biochimie* **1978**, *60*, 859–867.
(3) Faggiani, R.; Lippert, B.; Lock, C. J. L.; Rosenberg, B. *J. Am. Chem. Soc.* **1977**, *99*, 777–781.
(4) Stanko, J. A.; Hollis, L. S.; Schreifels, J. A.; Hoeschele, J. D. *J. Clin. Hematol. Oncol.* **1977**, *7*, 138–168.
(5) Lippert, B.; Lock, C. J. L.; Rosenberg, B.; Zvagulis, M. *Inorg. Chem.* **1978**, *17*, 2971–2975.
(6) Faggiani, R.; Lippert, B.; Lock, C. J. L.; Rosenberg, B. *Inorg. Chem.* **1978**, *17*, 1941–1945.
(7) Faggiani, R.; Lippert, B.; Lock, C. J. L.; Rosenberg, B. *Inorg. Chem.* **1977**, *16*, 1192–1196.
(8) Gill, D. S.; Rosenberg, B. *J. Am. Chem. Soc.* **1982**, *104*, 4598–4604.
(9) Macquet, J. P.; Cros, S.; Beauchamp, A. L. *J. Inorg. Biochem.* **1985**, *25*, 197.
(10) Cleare, M. J. *J. Clin. Hematol. Oncol.* **1977**, *7*, 1–25.
(11) Broomhead, J. A.; Fairlie, D. P.; Whitehouse, M. W. *Chem.-Biol. Interact.* **1980**, *31*, 113–132.

0020-1669/88/1327-0010$01.50/0